Time transfer using an asynchronous computer network: An analysis of error sources

S.C. Ebenhag, P. Jarlemark, P.O. Hedekvist, and R. Emardson
Measurement Technology and communication (MTk)
SP Technical Research Institute of Sweden
Borås, Sweden
Email: sven-christian.ebenhag@sp.se

***Abstract*—We have performed a time transfer over a distance of approximately 75 km using an asynchronous computer network based on optical fibers. In order to validate the results from this fiber-link, we have compared the results with a GPS-link, which consists of carrier phase observations. All electronic cabinets were equipped with temperature and humidity sensors. Here we present experiments where the temperature and humidity of the delay in the electrical components were investigated. All components showed some temperature dependence, but no significant humidity dependence was found. By using the derived temperature coefficient for the components the standard deviation of the difference between the fiber link and GPS link decreased from 243ps to184ps.**

I. INTRODUCTION

The time and frequency group of SP have performed a time transfer between clock locations SP (Borås) (node A) and Gothenburg (node C) using an active asynchronous computer network based on optical fiber. The only existing fiber between those two locations passes Borås City (node B). The time transfer distance is approximately 75 km. By passing Borås City the time transfer were forced to make a connection between two asynchronous fiber links. The connection was equipped with an extra oscillator which the two asynchronous links could be compared to. This test system was equipped with three clocks, one cesium and two rubidium, as shown in Fig. 1.

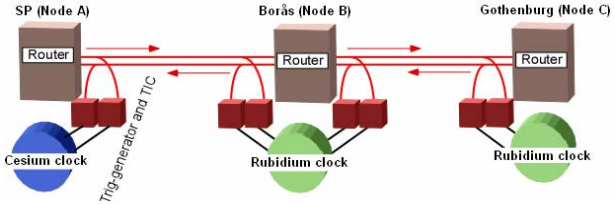

Figure 1. Clock comparison. The clocks in node A and node C can be compared using the signals going in both directions. Aproximate distance between node A and B is 5 km, and node B and C is 70 km.

One of the goals with this project is to develop a method to compare oscillators over long distances as a supplement to satellite-based transfer methods. In order to evaluate the system we used a GPS link based on the carrier phase changes. The result from this experiment is presented in [1]. For the purpose of evaluating and comparing error sources for the fiber-link and GPS-link used for time transfer, we equipped the electronic cabinets with temperature and humidity sensors. In addition, the outdoor temperature was recorded during the experiment. The outdoor temperature variations in this region during this period were 25 K and the indoor temperature variations in the proximity of the electronic equipment were 0.5 K to 2 K at different locations. The relative humidity varied some 40% at different locations. Two way measurements, schematically described in Fig. 1 were performed in order to compensate for changes in delay of the transmission in the optical fiber due to temperature changes. The derived variation of this delay is shown in Fig. 2.

After compensating for the measured transmission variations, the difference between the fiber-link and the GPS-link over a three-week experiment is shown in Fig. 3, with a standard deviation of 243ps.

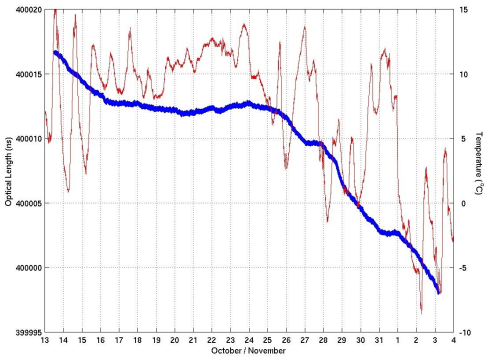

Figure 2. Optical length of the fiber between Borås and Gothenburg. The outdoor temperature at Gothenburg is shown in red.

This research is funded by The Swedish National Post and Telecom Agency (PTS) S.C. Ebenhag and P.O. Hedekvist are also affiliated with Chalmers University of Technology, Gothenburg, Sweden.

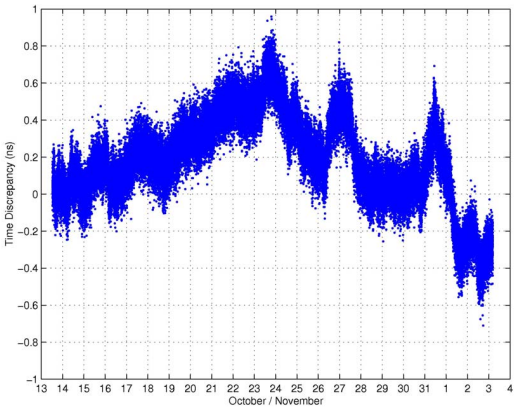

Figure 3. Difference between GPS-link and Fiber-link from 3 weeks of measurement.

The difference between the methods shows some systematic variations. These are correlated with the temperature measured among the electronics. Most of the variations are thus assumed to depend on these components. Therefore we performed an experiment in a climate chamber to evaluate the environmental dependence of the electronic components individually. The electronic components of the same category are assumed to have comparable temperature and humidity variations. The experiments were thus performed only with the electronic components from node C (Gothenburg).

II. ELECTRONIC COMPONENTS

The fiber system is built up from 1pps distribution, 10MHz distribution, Time Interval Counters (TIC), Optical Electrical converters (OE), Header Recognizer cards (HR) and computers. The GPS-link is built up from receivers, antennas and computers.

The fiber link split 1 and 10% of the light from the optical fiber. This light is converted into electrical signals in the OE-converter, and these signals are then decoded in the HR-card. When a frame is detected a pulse is produced and leaves the card into one of the time interval counters. The HR card produces a pulse every 125µs. In the TIC, a time interval is measured between the 1pps pulse from the oscillator which should be compared, and the pulse from the HR-card. The internal oscillators of the TICs are not sufficiently stable which is solved by connecting 10MHz reference through a 10MHz distribution. The 1pps pulse from the oscillator passes a 1pps distribution in order to serve the TICs.

In order to make a good comparison between the systems, both links must be evaluated. The GPS-link contains an antenna, antenna cable, receiver and a computer. Variations in the antenna and antenna cable are neglected in these experiments, based on results on the temperature dependence in the cable that previously have been evaluated [2]. Only the receiver is therefore left to be investigated.

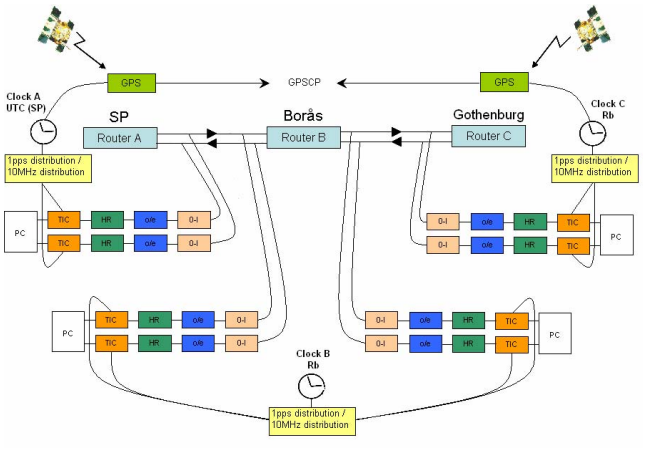

Figure 4. Example of a time transfer link with GPS as reference

III. EXPERIMENTAL METHODOLOGY

Temperature and humidity has been varied in a climate chamber for the purpose to evaluate the temperature sensitivity of the delay in the time transfer components. Fig. 5 and 6 shows the temperature and humidity algorithm for the climate chamber. The temperature was changed in step of 5 K and the humidity in steps of 10%.

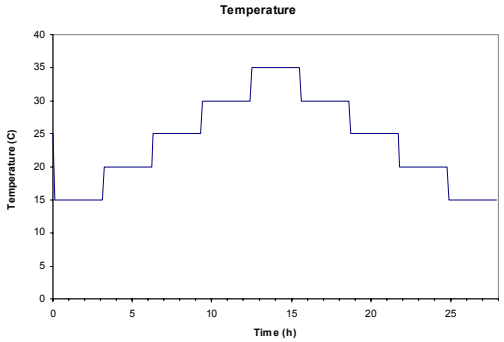

Figure 5. Temperature algorithm for the climate chamber

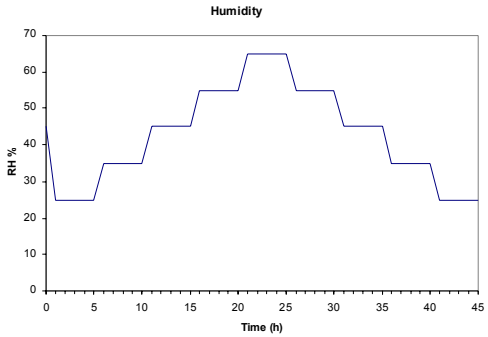

Figure 6. Humidity algorithm for the climate chamber

IV. EXPERIMENTAL RESULTS

Time interval measurements of the TIC, 1pps distribution, 10 MHz distribution, OE-converter, and HR card have been performed individually in order to evaluate the electrical components delay sensitivity due to temperature and humidity. All experiments showed measurable delay changes due to temperature however no influence of humidity was detected. Figs. 8, 10, 12, 14, 16 och 18 show the connection of the components during the different measurements. The noise in these experiments is large in comparison to the temperature dependence, and can be related to the TICs used in the measurements. Because of the noise the average values of every measurement has been calculated, to achieve the temperature coefficient for each electronic component.

A. TIC

Measurement coupling for evaluating temperature dependence of the TIC was made as shown in Fig. 7. The result of TIC evaluation shows the temperature dependence of the delay (Fig. 8). A temperature coefficient of 6,6ps/K was derived.

B. 10 MHz distribution

Measurement coupling for evaluating temperature dependence of the 10MHz distribution was made as shown in Fig. 9. The result of 10MHz distribution evaluation shows a temperature dependence of the delay (Fig. 10). A temperature coefficient of 2,7ps/K was derived.

C. 1pps distribution

Measurement coupling for evaluating temperature dependence of the 1pps distribution was made as shown in Fig. 11. The result of 1pps distribution evaluation shows a temperature dependence of the delay (Fig. 12). A temperature coefficient of 218,3ps/K was derived.

D. OE-converter

Measurement coupling for evaluating temperature dependence of the OE-converter was made as shown in Fig. 13. The result of OE-converter evaluation shows a temperature dependence of the delay, however as seen in Fig. 14, the delay will not decrease when the temperature decreases from 35 to 15 degrees C. This is likely due to internal heating of the component. Therefore we used only the first 20 hours of measurement to derive a temperature coefficient, which was calculated to 5,9ps/K.

E. HR-card

Measurement coupling for evaluating temperature dependence of the HR-card was made as shown in Fig. 15. The result of HR-card evaluation shows a temperature dependence of the delay (Fig. 16). A temperature coefficient of 2,3ps/K was derived.

F. GPS-receiver

Measurement coupling for evaluating temperature dependence of the GPS-receiver was made as shown in Fig. 17. The result of GPS-receiver evaluation shows a temperature dependence of the delay (Fig. 18). A temperature coefficient of 92,3ps/K was derived when phase measurement from the receivers were compared.

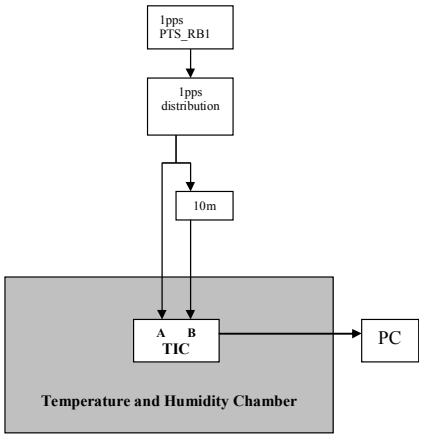

Figure 7. Measurement coupling for evaluating temperature dependence of time interval counter.

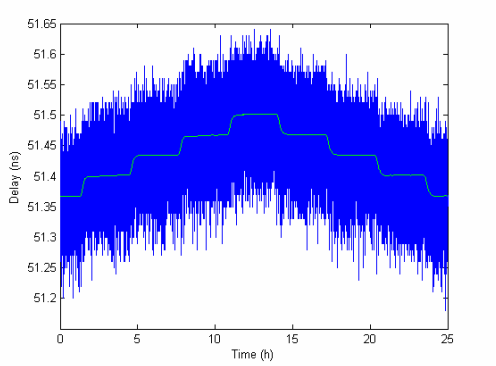

Figure 8. Results from experiment with TIC. In the result graphs the blue curves are the delay changes due to temperature in the components. The green curves show the temperature changes in the climate chamber (scaled to match the blue curves).

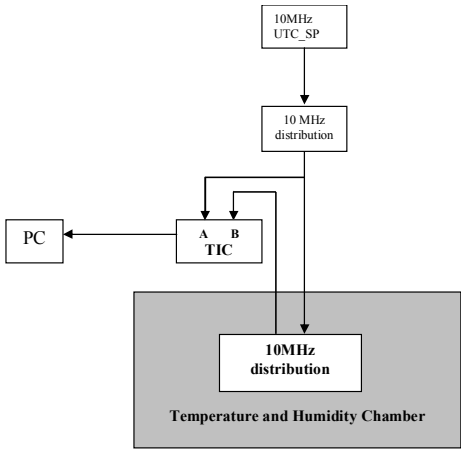

Figure 9. Measurement coupling for evaluating temperature dependence of 10MHz distribution.

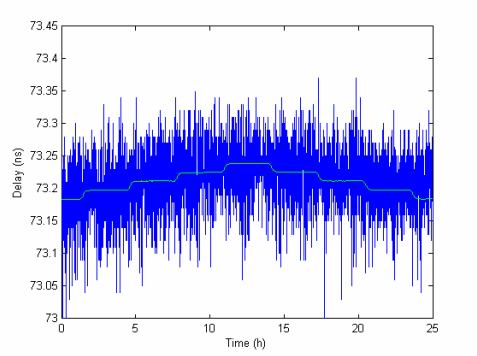

Figure 10. Results from experiment with 10MHz distribution. In the result graphs the blue curves are the delay changes due to temperature in the components. The green curves show the temperature changes in the climate chamber (scaled to match the blue curves).

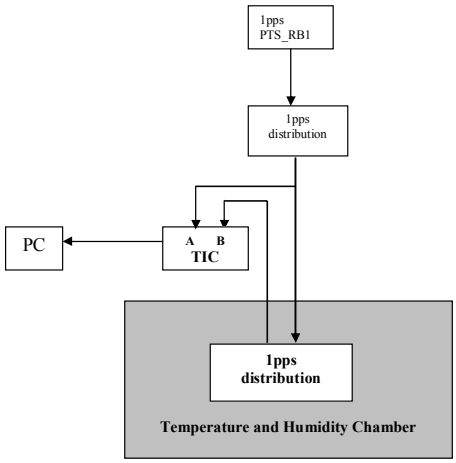

Figure 11. Measurement coupling for evaluating temperature dependence of 1pps distribution.

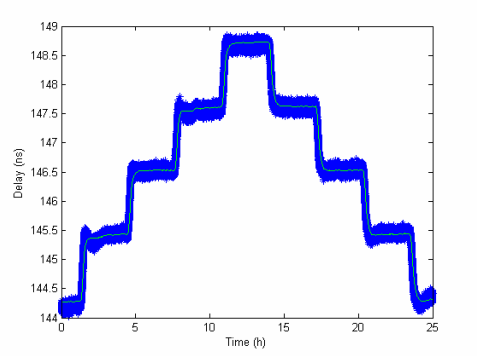

Figure 12. Results from experiment with 1pps distribution. In the result graphs the blue curves are the delay changes due to temperature in the components. The green curves show the temperature changes in the climate chamber (scaled to match the blue curves).

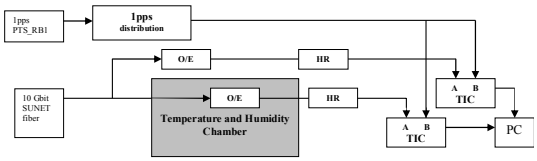

Figure 13. Measurement coupling for evaluating temperature dependence of OE-converter.

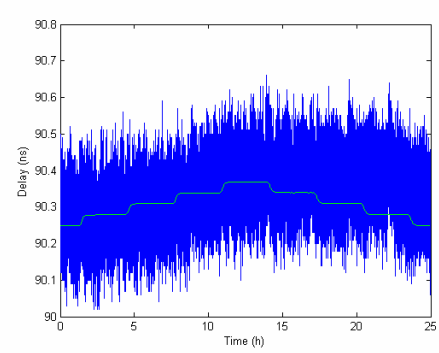

Figure 14. Results from experiment with OE-converter. In the result graphs the blue curves are the delay changes due to temperature in the components. The green curves show the temperature changes in the climate chamber (scaled to match the blue curves).

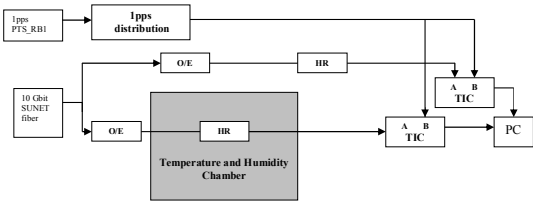

Figure 15. Measurement coupling for evaluating temperature dependence of HR-card.

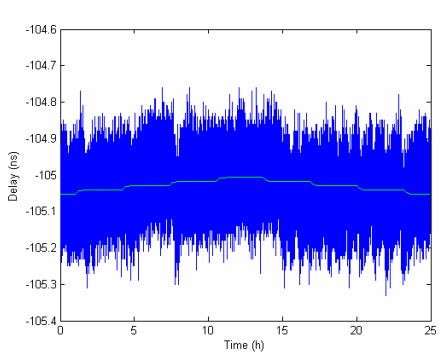

Figure 16. Results from experiment with HR-card. In the result graphs the blue curves are the delay changes due to temperature in the components. The green curves show the temperature changes in the climate chamber (scaled to match the blue curves).

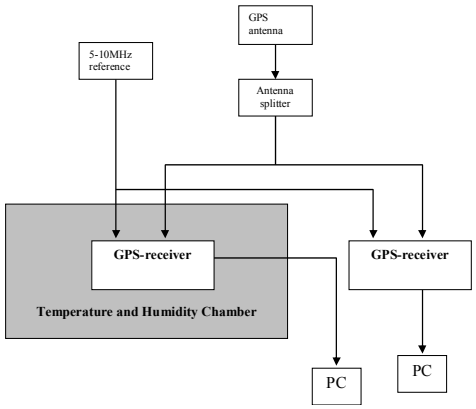

Figure 17. Measurement coupling for evaluating temperature dependence of GPS-receiver.

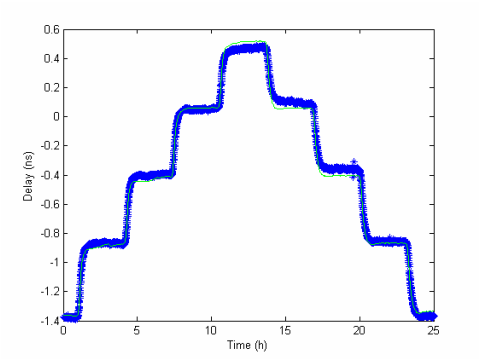

Figure 18. Results from experiment with GPS-receiver. In the result graphs the blue curves are the delay changes due to temperature in the components. The green curves show the temperature changes in the climate chamber (scaled to match the blue curves).

V. TEMPERATURE COMPENSATION

The difference between the GPS and Fiber link can now be compensated by using the temperature coefficient and the monitored temperatures. Using these data, a decrease of the standard deviation of the difference between the fiber and GPS link from 243ps to 184ps was estimated.

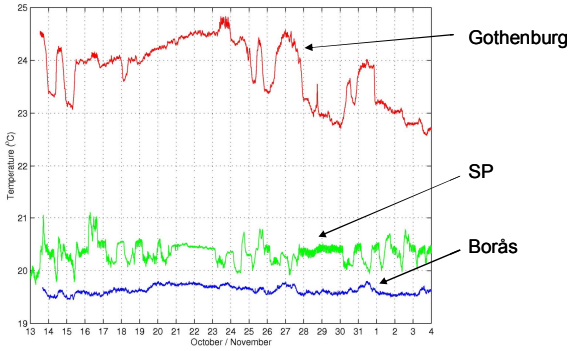

Figure 19. Temperature in the clock nodes from 3 weeks of measurement.

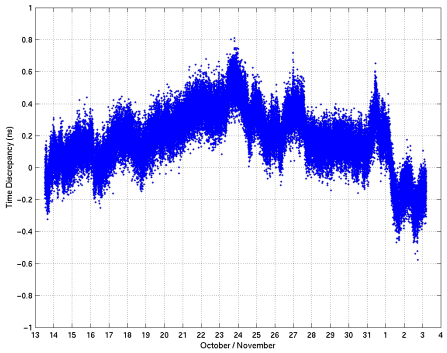

Figure 20. Difference between GPS-link and Fiber-link from 3 weeks of measurement with temperature compensation.

VI. CONCLUSION

The evaluation of the components has resulted in a decrease in the standard deviation of the difference between the fiber and GPS link from 243ps to 184ps. The remaining difference is probably caused in the fiber optics network due to different time delay. The major part is compensated for by the two way measurements, but residual effects are likely to remain due to mismatch between the directions. Large temperature dependency could get reduced by integrating the TICs into the Field Programmable Gate Arrays (FPGA) used on the HR-cards. This would also eliminate the need for separate components for the 1pps and 10MHz distributions.

VII. REFERENCES

[1] R. Emardson, P.O. Hedekvist, K. Jaldehag, M. Nilsson, and S.C. Ebenhag, P. Jarlemark, C. Rieck, J. Johansson, L. Pendrill, P. Löthberg, and H. Nilsson, "Time transfer using an asynchronous computer network: Results from three weeks of measurements", Proc. of the 21st European Frequency and Time Forum, paper 7169 (2007)

[2] C. Rieck, P. Jarlemark, K. Jaldehag and J. Johansson, "Thermal influence on the receiver chain of GPS carrier phase equipment for time and frequency transfer", Proc. of the 17th European Frequency and Time Forum. pp. 326 – 331, (2003)